

Supporting Information

Guillaumond et al. 10.1073/pnas.1421601112

SI Materials and Methods

Mouse Strains and Tissue Collection. We used male *Pdx1-Cre; Ink4a/Arf^{fl/fl}; LSL-Kras^{G12D}* mice, developing spontaneous PDAC, between 8 and 12 wk of age, and their mating control littermates, as previously described (1). After killing, pieces of tumor or control pancreas were fixed in 4% (wt/vol) formaldehyde or frozen in cold isopentane for further analysis, or directly homogenized in 4M guanidinium isothiocyanate lysis buffer for efficient pancreatic RNA extraction, according to Chirgwin et al.'s procedure (2).

Microarray Analysis. Expression array data (Mouse Transcriptome Assay 1.0, Affymetrix) were normalized with standard RMA (Bioconductor, Package Affy) and filtered from a precompiled Gene Ontology (GO) terms list, annotated with the term "metabolic" (National Center for Biotechnology Information GO-gene association file downloaded April 1, 2013; <ftp://ftp.ncbi.nlm.nih.gov/gene/DATA/gene2go.gz>), to restrain analysis to metabolic transcripts. A list of these metabolic transcripts is available upon request. Significant PDAC dysregulated transcripts and enriched pathways were determined by the Significance Analysis of Microarrays method (MeV software) and a Bonferroni-corrected hypergeometric distribution, respectively. Results can be accessed from the GEO database (www.ncbi.nlm.nih.gov/geo, accession no. GSE61412).

Human Tumor Collection and mRNA Extraction. Tumor specimens from 23 patients (54–79 y old) were taken, with their consent, during surgery (tissue collection: DC-2013-1857). A portion of each human tumor was fixed in 10% (wt/vol) formalin for histology analysis, and another portion was used for RNA isolation using the AllPrep DNA/RNA mini kit (Qiagen). RNA quality was verified on RNA Nano chips (Agilent). PDAC stages were classified according to the American Joint Committee on Cancer staging system. A post-operative follow-up, including clinical, biochemical, and radiological assessment, was performed for all patients.

Establishment of Stable shRNA PK4A Cell Lines. The 293T cells were cotransfected with lentiviral vectors expressing shRNA targeting LDLR (*Ldlr1*, clone ID: NM_010700.1-1457s1c1; *Ldlr2*, clone ID: NM_010700.1-2457s1c1; *Ldlr3*, clone ID: NM_010700.2-3407s21c1, *Ldlr4*, clone ID: NM_010700.1-1304s1c1; *Ldlr5*, clone ID: NM_010700.1-1864s1c1, *Ldlr6*, clone ID: NM_010700.2-1124s21c1 and clone ID: NM_010700.2-642s21c1; Sigma-Aldrich) or a nonmammalian control shRNA (SHC202V, Sigma-Aldrich), together with pCMV- δ helper and pCMV-VsVg plasmids, using lipofectamine 2000 (Invitrogen). PK4A cells (1.3×10^6), were infected twice at 24-h intervals with shRNA-expressing lentiviruses. Puromycin-selected cells were grown in glutamax high-glucose DMEM (Life Technologies), supplemented with 10% (vol/vol) FBS GOLD (PAA Laboratories), 1% antibiotic-antimycotic solution (Life Technologies), and puromycin (0.2 μ g/mL).

PDAC Syngeneic Graft Models. Under isoflurane anesthesia [induction: 4% (vol/vol) and maintenance: 1.5% (vol/vol)], 5-wk-old male NMRI nude mice (Harlan) were subcutaneously implanted between the shoulders with 2×10^6 control or *Ldlr3* shRNA PK4A cells. Two times each week, GEM (125 mg/kg; Lilly) was intraperitoneally administered and tumor size was determined with calipers. Tumor volume was established with the following formula: $(L \times W^2)/2$. Tumoral weight was determined at the experimental endpoint.

Cell Viability Assays. For cell viability assays, 1×10^5 *Ldlr* shRNA and control shRNA PK4A cells were plated in 12-well plates for

24 h before replacement of the standard medium with DMEM supplemented with 5% (vol/vol) FBS and 1% antibiotic-antimycotic solution. Cells were trypsinized after either 24, 48, or 72 h and live cells were determined by Trypan blue exclusion using the automated cell counter apparatus (Life Technologies) or cell viability analyzer (Vi-Cell, Beckman Coulter). The diameter of live cells was determined with Vi-Cell counter. Cell proliferation was monitored every hour for 80 h using the iCELLigence Sytem (ACEA Biosciences). Cell electrode impedance was expressed as an arbitrary unit called cell index and corrected for background impedance of the media alone.

Dil-LDL Uptake. Control and *Ldlr3* shRNA PK4A cells (1×10^6) were seeded in six-well culture plates and cultured in standard medium overnight. After 1 h of serum starvation, cells were incubated with Dil-LDL (5 μ g/mL; Molecular Probes) for 30 min. Trypsinized cells were then resuspended in $1 \times$ PBS and Dil-LDL uptake was analyzed in 1×10^4 cells using a MACSQuant VYB instrument (Miltenyi Biotec). Untreated cells were used as negative controls for background fluorescence.

Clonogenic Assays. For clonogenic assays, 8×10^2 control and *Ldlr3* shRNA PK4A cells were seeded into a 12-well plate and cultured in high glucose DMEM media with 10% (vol/vol) FBS and 1% antibiotic-antimycotic solution. Five days later, colonies were fixed in 10% (wt/vol) formalin, stained with 0.5% Crystal violet, imaged, and quantified by ImageJ software (NIH).

Cell Cytotoxicity Assay. For cell cytotoxicity assays, 8×10^4 control and *Ldlr3* shRNA PK4A cells (8×10^4), seeded in 96-well plates, were treated with GEM (Gemzar, Lilly), oxaliplatin (Hospira) (one-quarter dilution scheme: 1–1,000 nM) or with SN38 (Sigma-Aldrich, H-0165) (one-quarter dilution scheme: 0.1–100 nM) for 48 h. Cell viability was determined with PrestoBlue reagent (Life Technologies) and fluorescence intensity was measured with a microplate reader (TriStar, Berthold Technologies). The IC_{50} was calculated using a four parameter logistic non-linear regression with BioDataFit 1.02 software.

Cell Cycle Analysis. Control and *Ldlr3* shRNA PK4A cells (1×10^6) were fixed in 70% (vol/vol) ethanol. After RNA removal by RNase digestion (100 μ g/mL), cells were stained with propidium iodide (50 μ g/mL; Sigma-Aldrich) and analyzed by flow cytometry using a MACSQuant VYB instrument (Miltenyi Biotec). The cell number in each phase was determined using the Watson Pragmatic model with FlowJo software (Tree Star).

Cholesterol Assays. Total lipids from control or tumoral pancreas, control and *Ldlr3* shRNA -implanted tumors or control and *Ldlr3* shRNA PK4A cells were extracted according to the Bligh and Dyer method (3). FC and EC were separated by high-performance TLC (Camag) and quantified by scanning densitometry with a TLC Visualizer (Camag).

Glucose and Lactate Assays. Control and *Ldlr3* shRNA PK4A cells (1×10^5) were grown in high-glucose DMEM supplemented with 5% (vol/vol) FBS and 1% antibiotic-antimycotic solution for 24, 48, or 72 h. The concentrations of L-lactate and D-glucose (mmol/L) from cultured-cell supernatants were determined electro-enzymatically using an YSI 2950 Biochemistry Analyzer (Yellow Springs Instruments). Each metabolite concentration was normalized to viable cells number determined using the Vi-Cell cell counter (Beckman Coulter).

Doxorubicin Uptake. Control and *Ldlr3* shRNA PK4A cells (1×10^6) were seeded in six-well culture plates and cultured in standard medium overnight. Cells were then treated with doxorubicin (DOX, 1 mg/mL) for 15, 30, 60, 120, or 240 min. Trypsinized cells were then resuspended in $1 \times$ PBS and DOX uptake was analyzed in 1×10^4 cells using a MACSQuant VYB instrument (Miltenyi Biotec). Untreated cells were used as negative controls for background fluorescence.

Immunohistochemistry. Formalin-fixed, paraffin-embedded mouse PDAC sections (5 μ m) were deparaffinized in xylene and rehydrated through a series of graded ethanol concentrations. Antigen retrieval was performed at 95 °C in target retrieval solution (pH 6; Dako) before quenching endogenous peroxidase activity [3% (vol/vol) H_2O_2]. Tissue sections were then incubated with goat anti-LDLR antibody (R&D Systems, AF2255), rabbit cleaved caspase 3 (Cell Signaling Technology, 9661), or rat Ki67 antibodies (BioLegend, 652402) and immunoreactivity was visualized using the Vectastain ABC kit (PK-4001, Vector Laboratories) according to the manufacturer's protocol. Peroxidase activity was revealed using the liquid-DAB⁺ substrate chromogen system (Dako). Counterstaining with Mayer hematoxylin was followed by a bluing step in 0.1% sodium bicarbonate buffer before final dehydration, clearance, and mounting of the sections. Percentage of positive cleaved-caspase 3 or Ki67 areas in pancreatic tumors were determined from 20 \times magnification images ($n > 5$ per group) using ImageJ software.

Immunohistochemistry with an anti-human LDLR antibody (LifeSpan Biosciences, C193443) was performed on formalin-fixed and paraffin-embedded human PDAC sections using the Ventana Discovery XT automated stainer (Ventana Medical Systems) in the Pathology Department (Hôpital Nord, Marseille). Antigen retrieval was performed with CC1 buffer (Cell Conditioning 1; citrate buffer pH 6.0; Ventana Medical Systems).

Immunofluorescence. Cryostat tumor and control pancreas sections (8 μ m) were fixed in cold acetone and preincubated in blocking solution [3% (wt/vol) BSA, 10% (vol/vol) donkey serum]. Tissue sections were then incubated with primary antibodies, followed by incubation with Alexa fluor 568- or Alexa fluor 488-conjugated secondary antibodies (Molecular Probes; 1:500). Stained tissue sections were mounted using Prolong Gold Antifade reagent with DAPI (Life Technologies).

Filipin Staining. Frozen tissue sections (tumor or control pancreas) or *Ldlr3* shRNA PK4A cells were fixed in 4% (wt/vol) formaldehyde and incubated with 1.5 mg/mL glycine. A heat-induced antigen-retrieval step, in 10 mM Sodium citrate, 0.05% Tween 20, pH6, was performed for each tissue section.

Tissue sections were incubated overnight at 4 °C with filipin (200 μ g/mL; Sigma-Aldrich, F4767) and then with anti-Lamin A/C antibody (1:100; Cell Signaling Technology) for 1 h at room temperature. Lamin A/C staining was revealed with Alexa fluor 568-conjugated secondary antibody (Molecular Probes; 1:500). Tissue sections were mounted using Prolong Gold Antifade reagent without DAPI (Life Technologies).

Cells were stained 30 min with filipin (50 μ g/mL) and then incubated in Syto red fluorescent nucleic acid stains (1/20,000; Molecular Probes) for 10 min before to be mounted as described above. Filipin staining was viewed by fluorescence microscopy using a DAPI filter and green pseudocolor was assigned to it to improve reader visibility.

Western Blot. Whole-cell proteins (50–65 μ g per lane) were resolved by SDS/PAGE using a 10% (vol/vol) acrylamide gel and were transferred onto nitrocellulose membranes, which were then blocked in 5% (wt/vol) milk in PBS before being incubated overnight with primary antibodies. ECL protein detection (Milipore) was performed with a Fusion Fx7 chemiluminescent imager and the band intensities of the proteins of interest were determined by densitometry using ImageJ software (NIH) and were normalized to respective β -actin band intensities or to total protein stained with Amido black.

Primary Antibodies. Primary antibodies were: wide-spectrum KRT (Abcam, ab9377), E-cadherin (Invitrogen, 13–1900), N-cadherin (Hypermatrix, HM1049), LDLR (R&D systems, AF2255), HMGCR (Santa Cruz Biotechnology, sc-33827), pERK1/2 (Sigma-Aldrich, M8159), ERK1/2 (Sigma-Aldrich, M5670), pMEK1/2 (Cell Signaling Technology, 2338), MEK1/2 (Cell Signaling Technology, 4694), MKP-3 (Santa Cruz Biotechnology, sc-8599), Lamin A/C (Cell Signaling Technology, 2032), and β -actin (Sigma-Aldrich, A5316).

PathScan Signaling Antibody Array Analysis. An antibody array for simultaneous detection of 18 well-characterized intracellular signaling molecules was used (Cell Signaling Technology, 7323). Control and *Ldlr3* shRNA PK4A cells were washed with ice-cold $1 \times$ PBS and lysed in the $1 \times$ Cell Lysis buffer provided. Total protein extracts were then hybridized, to the slide containing pre-spotted target-specific antibodies, overnight at 4 °C. A mixture of biotinylated detection antibodies was then added to each well and incubated for 1 h at room temperature and HRP-conjugated streptavidin was then added for 30 min. The slide was covered with the LumiGLO/Peroxide reagent provided and chemiluminescent signals were detected with a Fusion Fx7 imager.

Reverse-Transcript PCR and Quantitative PCR. Before reverse transcription, RNA quality was verified with the RNA Nano Chip kit (Agilent) on an Agilent Bioanalyzer and treatment with DNase was systematically performed using the RNase-free DNase set (Qiagen). Then, 5 μ g of total RNA from each sample was used to synthesize the first-strand cDNA by using the PrimeScript RT reagent kit (Promega) and the provided oligo-dT primers, according to the manufacturer's instructions. Quantitative PCR reactions were performed with specific primers (Table S1) and the GoTaq qPCR master mix kit (Promega) using the Mx3005P Stratagene system. Differential expressions of transcripts of interest were calculated in relation to the *Rplp0* housekeeping transcript.

Statistical Analysis. Significant differences between two experimental groups were determined using the Mann–Whitney *U* test or *t*-test. One-way ANOVA was used to compare more than two experimental groups followed by Tukey's HSD post hoc tests (Real Statistics). All data are expressed as mean \pm SEM or SE and statistical significance was defined as ^a**P* < 0.05. The patient cohort was separated in two groups, based on the levels of *Ldlr* expression in tumors (high- and low-*Ldlr* expression groups) using a maximally selected rank statistics test to maximize the *P* value (<0.05) of the overall and disease-free survival Kaplan–Meier models. Overall survival refers to the survival time between date of surgery and the last follow-up time or death date, and disease-free survival refers to the time a patient survives without evidence of the disease. The start-point is the date of surgery and the end-point is the recurrence date, the last follow-up time, or death date.

- Guillaumond F, et al. (2013) Strengthened glycolysis under hypoxia supports tumor symbiosis and hexosamine biosynthesis in pancreatic adenocarcinoma. *Proc Natl Acad Sci USA* 110(10):3919–3924.
- Chirgwin JM, Przybyla AE, MacDonald RJ, Rutter WJ (1979) Isolation of biologically active ribonucleic acid from sources enriched in ribonuclease. *Biochemistry* 18(24):5294–5299.

- Bligh EG, Dyer WJ (1959) A rapid method of total lipid extraction and purification. *Can J Biochem Physiol* 37(8):911–917.

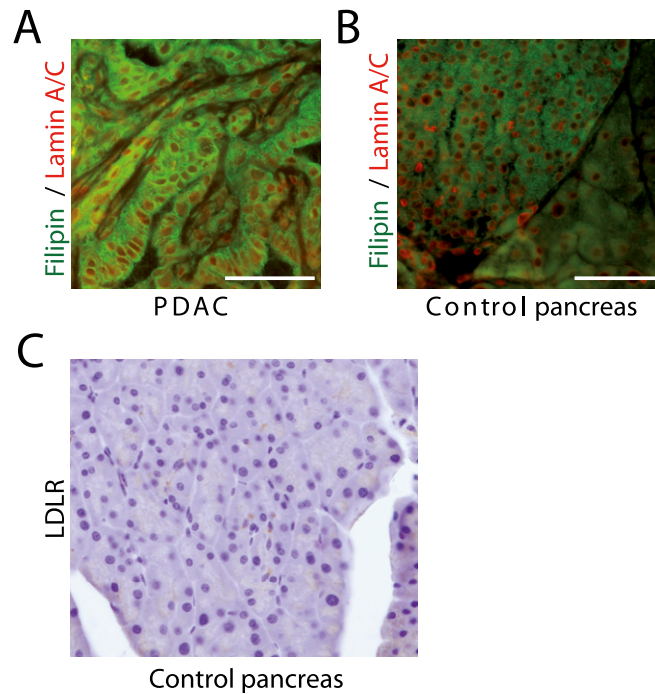


Fig. S1. Filipin-stained FC in PDAC (A) and control pancreas (B). Lamin A/C are used to stain nucleus membranes. Green pseudocolor, instead of blue, was assigned to filipin to improve reader visibility. Magnification: 40 \times and 20 \times , respectively. (Scale bars, 100 μ m.) (C) LDLR protein expression in control pancreas. Magnification: 20 \times .

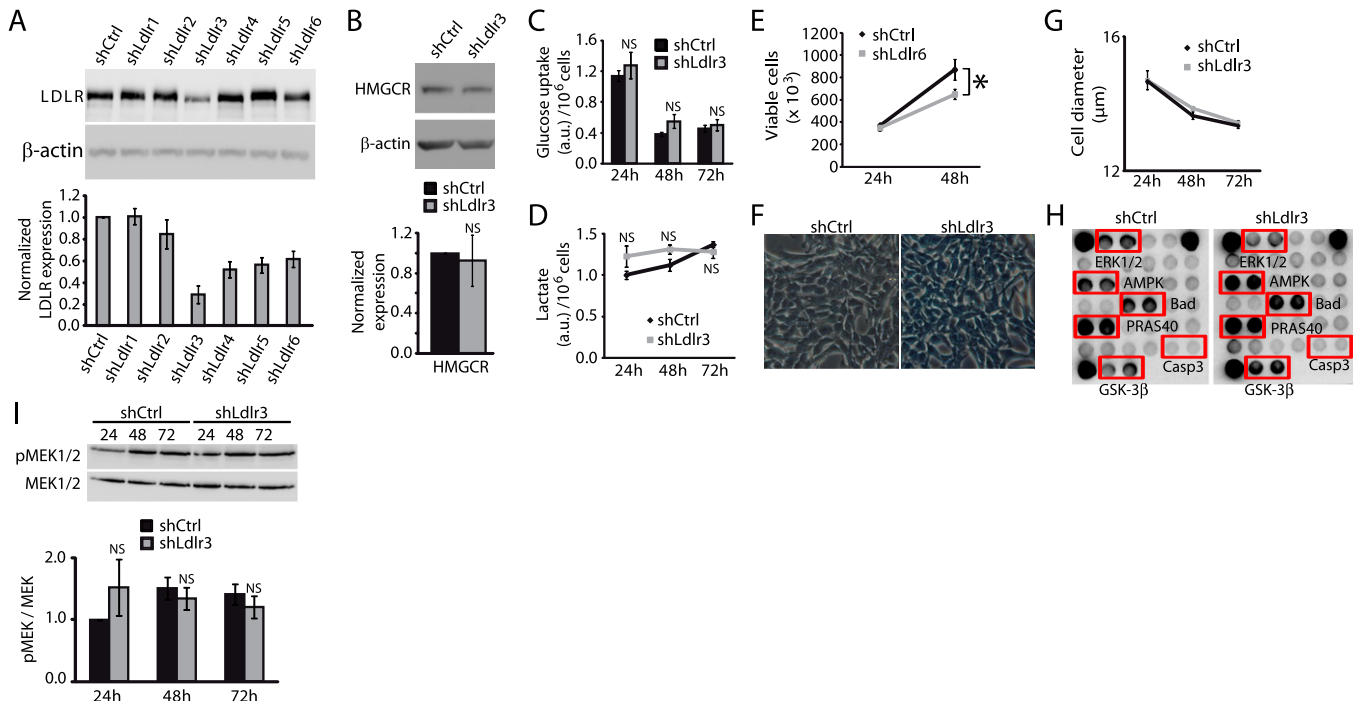


Fig. S2. LDLR silencing disturbs pancreatic cancer cell proliferation without inducing compensatory processes as an overactivation of the cholesterol synthetic pathway. (A) LDLR protein expression in PK4A cell lines expressing shRNA, targeting different *Ldlr* sequences (sh*Ldlr1-6*) related to that determined in non-mammalian shRNA control (shCtrl) cells. β -Actin protein expression is used as loading control. (B) HMGCR protein expression in shCtrl and sh*Ldlr3* PK4A cells and normalized as in A. Glucose uptake (C) and lactate production (D), determined from shCtrl and sh*Ldlr3* PK4A supernatant every 24 h over a 72-h period, and normalized to respective viable cell number. (E) The number of viable shCtrl and sh*Ldlr6* PK4A cells after 24 and 48 h in culture. * $P < 0.05$, ANOVA, $n = 3$. (F) Bright-field images of shCtrl and sh*Ldlr3* PK4A cells. Magnification: 20 \times . (G) Diameter of shCtrl and sh*Ldlr3* PK4A cells determined every 24 h over a 72-h period. (H) Representative pathscan intracellular signaling arrays performed upon shCtrl and sh*Ldlr3* PK4A protein extracts. Proteins of interest are framed in red. (I) pMEK1/2 proteins expression, normalized to MEK1/2 protein levels, in shCtrl and sh*Ldlr3* cells grown over 24, 48, and 72 h. (A–E, G, I) Data are plotted as mean \pm SEM Student's *t* test or ANOVA, $n = 3$ individual experiments. For all panels, the shCtrl and sh*Ldlr3* abbreviations are used for control and *Ldlr3* shRNA PK4A cells, respectively. Nonsignificant (NS) and * ($P < 0.05$) are relative to control shRNA PK4A values.

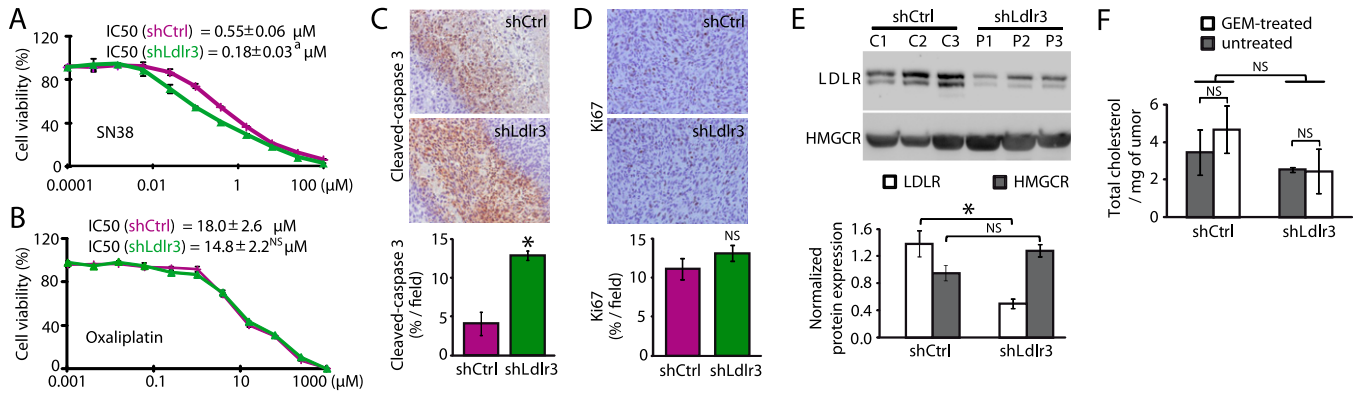


Fig. 53. Disruption of LDLR alters the sensitivity of PDAC cells to drugs without affecting cholesterol synthesis or content in tumors. Cytotoxicity dose-response curves for SN38 (A) and oxaliplatin (B) performed on shCtrl and *shLdlr3* PK4A cells, 48 h after starting treatment. The cell viability is expressed as a percentage of untreated cells. The IC_{50} of the drug, determined for each cell line, is indicated. Means represent at least three independent experiments. Cleaved-caspase 3 (C) and Ki67 (D) staining in shCtrl and *shLdlr3* implanted tumors. Magnification: 20 \times . Quantification of positive-stained area in shCtrl and *shLdlr3* implanted tumors is illustrated ($n > 5$ per tumor), $*P < 0.05$. (E) LDLR and HMGR proteins expression in shCtrl (C1–C3) and *shLdlr3* (P1–P3) implanted tumors. Mean protein levels in each tumor are normalized to total loaded-protein (Amido black staining). $*P < 0.05$. (F) TC quantities in shCtrl- and *shLdlr3*-implanted tumors measured per milligrams of tissue ($n = 5$ per group). NS, nonsignificant.

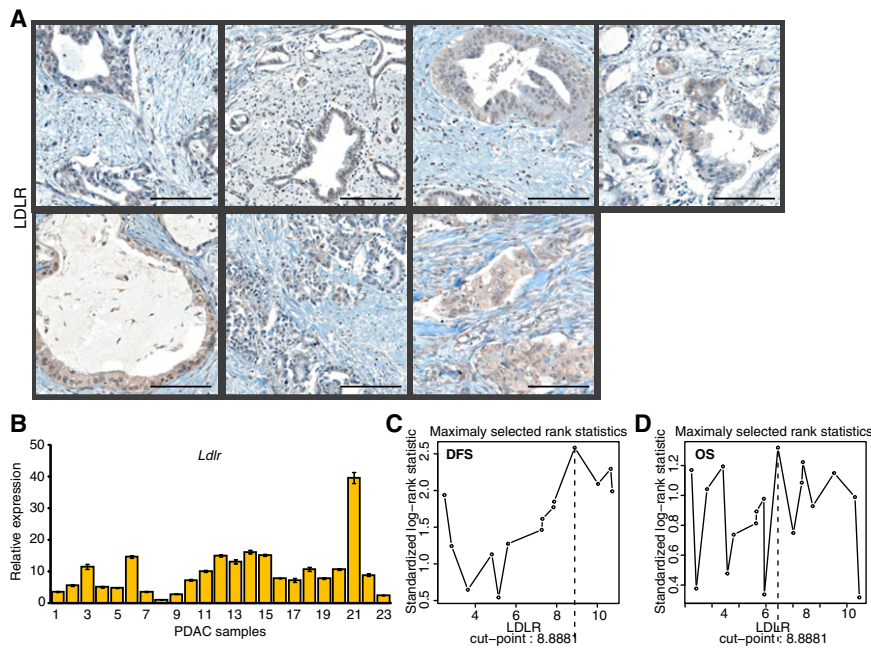


Fig. 54. Localization of LDLR in human PDAC and expression of its transcripts relative to stage of PDAC. (A) LDLR protein expression in seven human PDAC collected during surgery. Magnification: 20 \times . (Scale bars, 100 μ m.) (B) *Ldlr* transcript expression in 23 other human PDAC, determined by quantitative real-time PCR and normalized to *Rplp0* mRNA levels. Data are expressed as mean \pm SEM ($n = 3$). (C) Cut-off points, relative to disease-free survival (DFS) and (D) overall survival (OS), determined using maximally selected rank statistic test, which allow partition of the patient cohort into low- and high-*Ldlr* expression groups.

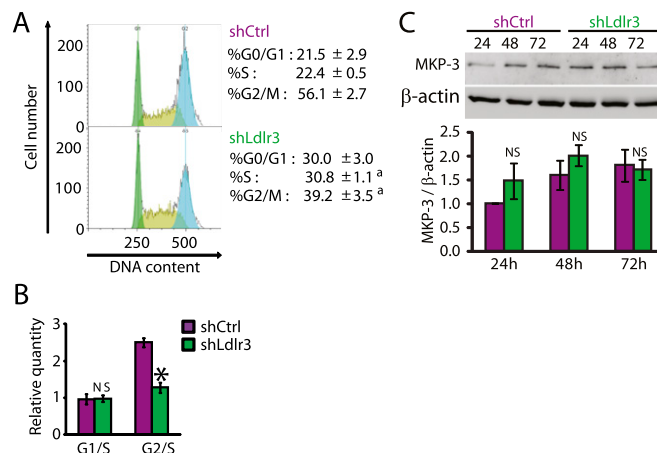


Fig. 55. LDLR suppression prevents cell-cycle progression into the G₂/M phase and does not alter MKP-3 phosphatase activity. (A) Flow cytometry cell cycle analysis of shCtrl and shLdlr3 PK4A cells stained with propidium iodide. Representative cell-cycle plots and percentage of each indicated cell line in G₀/G₁, S, and G₂/M phases are illustrated. ^a*P* < 0.05. (B) Relative G₁/S and G₂/S ratios calculated from shCtrl and shLdlr3 PK4A cells. **P* < 0.05. (C) MKP-3 protein expression, normalized to β-actin protein levels, in shCtrl and shLdlr3 cells grown over 24, 48, and 72 h. Data are mean ± SEM and represent at least three independent experiments. NS, Nonsignificant is relative to control shRNA values.

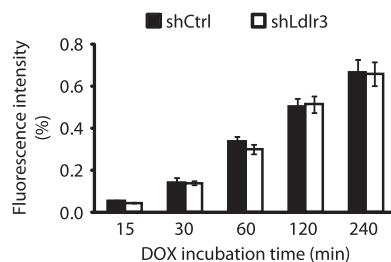


Fig. 56. DOX uptake is not affected by LDLR silencing. Cellular uptake of DOX in shCtrl and shLdlr3 PK4A cells after the indicated time of incubation with DOX and determined by flow cytometry.

Table S1. Primer sequences used to determine transcript expression profiles by real-time PCR

| Gene name | Species | Forward primer sequence (5'-3') | Reverse primer sequence (5'-3') |
|-----------------|---------------------|---------------------------------|---------------------------------|
| <i>Hmgcr</i> | <i>Mus musculus</i> | GGTCCAAGTACATTCTGGGTATT | AAAAAGGGCAAAGCTTCATTT |
| <i>Hmgcs1</i> | <i>Mus musculus</i> | AAGACGCCACACCAGGATCT | TGAGCTTCATGTTTCAGCAA |
| <i>Sc4mol</i> | <i>Mus musculus</i> | GGCTCCCTGATAGTTCACGA | GAAGGTTTCTGGTTTATCCTTTTG |
| <i>Nsdhl</i> | <i>Mus musculus</i> | GAGGCCGGAGTTCAGAAAC | TCAATAGGCTTCATGGCGTA |
| <i>Dhcr24</i> | <i>Mus musculus</i> | GTGGACACCAAGAAAACAGATTG | TCATCAAGCTCAGGCAACAC |
| <i>Acat1</i> | <i>Mus musculus</i> | ATTCTGACTGGAACAGATTTCG | TGGGTAGTGGATCTTTGCTTG |
| <i>Ch25h</i> | <i>Mus musculus</i> | TAAAGCAGCTTCTGCCTTGC | TGACTTAGGAGCTGGACGAG |
| <i>Hsd17b7</i> | <i>Mus musculus</i> | GGAAGTCAAGCAAAAAGTTTCA | AAAGATGCCGCAGAAAAATG |
| <i>Srd5a1</i> | <i>Mus musculus</i> | CCTGTTTCTGACAGGCTTT | ATCCAGTTTCCCCTGGTTTT |
| <i>Hsd17b12</i> | <i>Mus musculus</i> | CCGACTTGGACAACACCAT | CCACTGGCTGAGGAGATGTT |
| <i>Ldlr</i> | <i>Mus musculus</i> | CCATCAAGGAGTGCAGACC | CTGGGACACAGGCACTCAGA |
| <i>ApoE</i> | <i>Mus musculus</i> | CTGACAGGATGCTAGCCG | CGCAGGTAATCCCAGAAGC |
| <i>Lipa</i> | <i>Mus musculus</i> | GTCTGGCCCTTCAGTTTTG | GCCTTGAGAATGACCCACAT |
| <i>Rplp0</i> | <i>Mus musculus</i> | GCTGATGGCAAGAACACCA | CCCAAAGCCTGGAAGAAGGA |
| <i>Ldlr</i> | <i>Homo sapiens</i> | GGATCCGTTTCATGGCTTCA | ATTGGGCCACTGAATGTTTT |
| <i>Rplp0</i> | <i>Homo sapiens</i> | AATCCCTGACGCACC GCCGTGATG | TGGTTGTTTTCCAGGTGCCCTCG |

Other Supporting Information Files

- [Dataset S1 \(XLSX\)](#)
- [Dataset S2 \(XLSX\)](#)
- [Dataset S3 \(XLSX\)](#)